

ound [7]. At low ultrasound pressures, MBs ymmetric manner resulting in acoustic backe quality of the diagnostic image [8]. Exposure y ultrasound can also facilitate a phenomenon on which causes a transient 'poration' of cellular nd the phenomenon is enhanced in the presence of MBs. Such an approach has been exploited to enof gemcitabine therapy in pancreatic cancer patients st, at higher acoustic pressures, collapse of the MB and release of the shell fragments at the target site ure has been exploited by several groups investigating of MBs as targeted delivery vehicles [12,13]. In our prewe attached the antimetabolite drug 5-fluouracil (5-FU) osensitiser Rose Bengal (RB) to the shell of oxygen-loaded ised MBs for the combined antimetabolite and sonodynamic SDT) treatment of pancreatic cancer [6]. Significant reducthe viability of three pancreatic cancer cell lines (BxPC3, Ca-2 and Panc-01) and inhibition of the growth of ectopic panc BxPC-3 tumours were observed for the combined treatment n compared to either treatment alone. Antimetabolite therapy is an ablished treatment protocol for pancreatic cancer with 5-FU and emcitabine among the most commonly used antimetabolite drugs [14]. In contrast, SDT is an emerging anti-cancer treatment that involves the activation of an otherwise inactive sensitiser drug using lowintensity ultrasound [15]. The combination of sensitiser and ultrasound, in the presence of molecular oxygen, generates cytotoxic levels of reactive oxygen species (ROS) causing cell death via oxidative stress [16]. As oxygen is a key substrate for the generation of ROS in SDT, and since pancreatic adenocarcinoma is characterised as extremely hypoxic, providing oxygen during SDT can improve the ROS yield and enhance the therapeutic outcome [17]. While our oxygen carrying MBs have shown great promise as a platform for targeted oxygen delivery and enhanced 5-FU/SDT treatment of pancreatic cancer, there remains a need to demonstrate the effectiveness of this method in an orthotopic tumour model following intravenous injection of the MB suspension. To this end, we have reasoned that an additional layer of targeting may be required to help retain MBs in the tumour vasculature after injection and enhance the quantity of MBs destroyed at the target site by ultrasound exposure. The incorporation of magnetic nanoparticles within the MB shell is one approach that has been explored to improve the targeting capability of MBs [18]. Previous work in our laboratory has demonstrated that externally applied magnetic fields may be used to enhance the retention of magnetically-responsive microbubbles at a target site in an ex vivo model under physiologically-relevant flow rates [19]. In this manuscript, we assess the ability of oxygen loaded magnetic MBs with 5-FU and Rose Bengal attached to their surface, as a targeted treatment for orthotopic human pancreatic BxPC-3 tumours in SCID mice. The benefit afforded by incorporating magnetic targeting into our delivery platform is demonstrated by studies in a flow-phantom and by therapeutic efficacy studies in vivo.

### 2. Materials and methods

### 2.1. Reagents and equipment

1,2-dibehenoyl-sn-glycero-3-phosphocholine (DBPC) and 1,2-distearoyl-sn-glycero-3-phosphoethanolamine-N-[methoxy(polyethylene glycol)-2000] (DSPE-PEG(2000)) and DSPE-PEG(2000)-biotin were purchased from Avanti Polar Lipids (Alabaster, Alabama, USA). Oxygen gas was purchased from BOC Industrial Gases UK and perfluorobutane

study was preferred over the stabilised SPION as the addition of lipids to lipid-snene is likely to be less disruptive to the acoustic response of the system compared to the addition of isoparaffin [19]. These microbubbles have been extensively characterised and successfully used in previous in vivo experiments [20]. The method for magnetic microbubble fabrication used in this study has then been adapted for the use of lipid conjugated SPION: fluidMAG-Lipid as presented in the following section. MBs were formed using a Microson ultrasonic cell disruptor, 100 W, 22.5 kHz, from Misonix Inc. (NY, USA). Optical microscope images were obtained using a Leica DM500 optical microscope. MB concentration and size were determined using purpose- written MATLAB software (2010B, MathWorks, Natick, MA, USA). Rose Bengal sodium salt, NHS-biotin, MTT assay kit, avidin, chloroacetic acid, 4-dimethylaminopyridine (DMAP), hydroxybenzotriazole (HOBt), N,N'-dicyclohexylcarbodiimide (DCC), anhydrous dimethylformamide (DMF), and ethanol were purchased from Sigma Aldrich (UK) at the highest grade possible. Biotin, 5flurouracil, di(N-succinimidyl) carbonate and 2-aminoethanol were purchased from Tokyo Chemical Industry UK Ltd. Error was expressed as  $\pm$  SEM (standard error of the mean) and statistical comparisons were established using ANOVA and un-paired Student's t-test.

# 2.2. Preparation of avidin functionalised magnetic microbubbles (MagPFBMBs)

Avidin functionalised magnetic MBs were prepared by dissolving DBPC (4.0 mg, 4.43 µmol), DSPE-PEG(2000) (1.35 mg, 0.481 µmol) and DSPE-PEG(2000)-biotin (1.45 mg, 0.481 µmol) at a molar ratio of 82:9:9 in chloroform (274 µL). The chloroform solvent was slowly evaporated by heating the lipid solution at 40 °C overnight to produce a dried lipid film. The lipid film was reconstituted in 2 mL of a PBS (pH 7.4  $\pm$  0.1):propylene glycol:glycerol (8:1:1 v/v) mixture and the contents heated at 80 °C under stirring for 30 min in a water bath. FluidMAG-Lipids NPs (150 µL) were then added to the solution and the mixture was sonicated with a handheld sonicator probe for 1.5 min (100 W, 22.5 kHz, power setting 4). The headspace of the glass vial was then filled with perfluorobutane gas (PFB) and the gas/liquid interface was sonicated for 20 s (power setting 19), producing PFB-containing magnetic MBs (MagPFBMBs). The vial was immediately sealed and placed in an ice bath for 10 min. The MagPFBMB suspension was then centrifuged (100 RCF, 5 min) to remove the excess NPs and non-incorporated MB lipids by discarding the infranatant. The microbubble was re-suspended in 2 mL (pH 7.4 ± 0.1):propylene glycol:glycerol (8:1:1 v/v), avidin in PBS (50  $\mu$ L, 10 mg/mL) was added to the suspension and the contents mixed for 10 min on a rotary shaker. The suspension was centrifuged (100 RCF, 5 min) to remove the excess avidin and the PFBMBs were again resuspended in 2 mL of PBS (pH 7.4 ± 0.1):propylene glycol:glycerol (8:1:1 v/v). MagPFBMBs were analysed using a Leica DM500 optical microscope to obtain the size distribution and concentration. For this,  $10 \, \mu L$  of suspension was diluted in  $190 \, \mu L$  of PBS and examined using a haemocytometer (Bright-Line, Hausser Scientific, Horsham, PA, USA). 30 images were obtained with a  $40 \times$  objective lens and analysed with customised image analysis package in MATLAB (2010B, MathWorks, Natick, MA, USA). The iron content in the MagPFBMBs was determined by atomic absorption spectroscopy using a Varian fast sequential atomic absorption spectrometer. A calibration curve was constructed using known concentrations of Fe(III) in 0.5 M HCl. Readings were taken at 248.3 nm, 0.5 nm slit width, 10.0 mA lamp current, with the following flame settings; flame type: air/acetylene, air flow: 13.50 L/

MB-Rose Bengal and MagO<sub>2</sub>MB-5FU conjugates

tin functionalised Rose Bengal [16] and biotin have been described by us in previous comd solutions of biotin-RB and biotin 5-FU were v/v) DMSO: PBS (pH 7.4  $\pm$  0.1) solvent mixture. U and biotin-RB were added to separate samples gPFBMBs and allowed to mix for 5 min on a rotary ples were centrifuged (100 RCF, 5 min) to remove al and PFBMB conjugates were re-suspended in 1 mL of H 7.4  $\pm$  0.1). This conjugation/centrifugation process three times. The final PFBMB-RB and PFBMB-5FU contransferred to glass vials. MagO2MB-RB and MagO2MBates were obtained by sparging the MagPFBMB-RB and B-5FU with pure O<sub>2</sub> gas for 2 min and sealing the vial via A small sample (100 μL) of both the MagO<sub>2</sub>MB-RB and Ma-5FU conjugates was retained and the MB number again counted a haemocytometer. The remaining sample was sonicated in an onic bath for 5 min to burst the MBs and the Rose Bengal and 5concentration determined using UV-Vis (ultra violet - visible) ctroscopy and HPLC (high performance liquid chromatography) spectively [21].

### 2.4. Retention of MagMBs in a flow cell using an external magnetic field

MagPFBMBs without payload were used in this study to reduce wastage of biotin-5FU and biotin-RB.  $1 \times 10^7$  MagPFBMBs were placed in a 1 mL syringe, connected to an ibidi µ-Slide VI flow chamber using silicone tubing (1.6 mm internal diameter) and placed in a peristaltic syringe pump. A single N52 grade NdFeB permanent magnet cube (12.7 mm) with an internal magnetization of  $1.14 \times 10^6$  A/m was positioned 1 mm from the base of the flow chamber. Values for a field of 0.46 T and gradient of 83.1 T/m inside the flow chamber were calculated using a model described and experimentally verified previously [22], whereby the field was determined by breaking the magnet into a 3-dimensional lattice of evenly-distributed point moments, and summing the contributed dipole field from each moment. The MagPFBMBs were pumped through the flow chamber at a rate of 0.6 mL/min. Once the syringe was empty, the magnetic field was removed and 1 mL of PBS (pH 7.4  $\pm$  0.1) added to the syringe to flush the flow chamber's content into a clean vial. Collected MBs were counted using the method described above. As a control, the experiment was repeated in the absence of a magnetic field but under otherwise identical conditions. The number of MBs collected during the PBS flush was again recorded.

### 2.5. In vitro cell viability

Human primary pancreatic adenocarcinoma cell lines Mia PaCa-2 and Panc-1, were maintained in DMEM medium. The mouse primary pancreatic adenocarcinoma T110299 derived from a GEM mouse (KPC and a gift from Prof. J. Siveke, Technical University of Munich, Germany), was also maintained in DMEM medium while the human primary pancreatic adenocarcinoma cell line BxPc-3 was maintained in RPMI-1640 medium, all of which were supplemented with 10% (v/v) foetal bovine serum and grown in a humidified 5% CO<sub>2</sub> atmosphere at 37 °C. These cells were plated into the wells of a 96-well tissue culture plate at a concentration of 5  $\times$  10 $^3$  cells per well and incubated for 24 h at 37 °C in a humidified 5% CO<sub>2</sub> atmosphere. The media was then removed from each well and replaced with 100  $\mu$ L of treatment suspension and 100  $\mu$ L of fresh medium. This resulted in a final MB count and

ultrasound for 30 s, using a frequency density of 3.0 W cm $^{-2}$  (I<sub>SATP</sub>; spatial average, temporary sponding to a peak to peak pressure of 0.8 MPa in water and 0.5 MPa inside the well as measured with a needle hydrophone (Precision Acoustics, Dorset, UK); and a duty cycle of 50% (pulse frequency = 100 Hz). The solution was then removed from the wells and fresh medium added (200  $\mu L$ ). Plates were incubated in a humidified 5% CO $_2$  atmosphere at 37 °C for 21 h and cell viability determined using an MTT assay [23]. Results were compared with those obtained using untreated cells and cells exposed to ultrasound treatment alone.

### 2.6. Treatment of orthotopic BxPC-3 Luc tumours in SCID mice

All animals employed in this study were treated humanely and in accordance with licenced procedures under the UK Animals (Scientific Procedures) Act 1986. BxPc-3 Luc cells were maintained in RPMI-1640 medium supplemented with 10% foetal calf serum as described above. Cells (1  $\times$   $10^6)$  were re-suspended in 100  $\mu L$  of Matrigel® and orthotopically implanted into the head of the pancreas of female Balb/c SCID (C·B-17/IcrHan®Hsd-Prkdcscid) mice. 19 days after implantation, animals were randomly distributed into 3 groups (n = 4). Following induction of anaesthesia (intraperitoneal injection of Hypnorm/ Hypnovel), a  $100\,\mu L$  mixture of PBS containing MagO<sub>2</sub>MB-RB/ MagO<sub>2</sub>MB-5FU (MB =  $1.6 \times 10^8$ , [RB] =  $350 \,\mu\text{M}$  and [5-FU] =  $700 \,\mu\text{M}$ ) was administered by tail vein injection to Groups 2 & 3while Group 1 received vehicle only. For Group 2, ultrasound (frequency = 1 MHz, ultrasound power density =  $3.5 \,\mathrm{Wcm}^{-2} \,\mathrm{I}_{\mathrm{SATP}}$ ; spatial average temporal peak, corresponding to a free field peak to peak pressure of 0.85 MPa, duty cycle = 30% and pulse repetition frequency = 100 Hz) was directed to the tumour region (determined using prior bioluminescent imaging) via the abdomen for 3.5 min during and after injection (3.5 min total). For Group 3, in addition to ultrasound using the above parameters, a stack of permanent magnet discs (arranged to deliver the optimal magnetic force to the tumour region) [24] was directed to the tumour region (again via the abdomen) for 3.5 min during and after injection (3.5 min total), resulting in an approximate magnetic field at the tumour of 0.10 T and gradient 14.9 T/m. Treatments using the above conditions were repeated on Days 20 and 21 with animals sacrificed on Day 28. Tumours were then surgically excised and tumour volumes determined by direct measurement.

## 2.7. Determination of apoptotic marker expression in tumours post treatment

Following the determination of tumour volume a single cell suspension was prepared from the excised tumours. This involved homogenising the tumour tissue in 4% FCS in RPMI 160  $\mu L$  (30 mg/mL) collagenase type II, 50  $\mu L$  (2  $\mu g/mL$ ) DNAse and stirring for 15 min at room temperature. A further 160  $\mu L$  of collagenase II was subsequently added and the contents stirred for a further 15 min. The mixture was filtered through a 100  $\mu m$  filter, centrifuged at 1700 rpm for 5 min and re-suspended in 1 mL of Red Cell Lysis Buffer (RCLB) for 10 min. RCLB was neutralised by adding media containing FCS and cells were recovered by centrifuging at 1700 rpm. The pellet was washed twice with PBS, centrifuged and re-suspended in 700  $\mu L$  PBS buffer. For BAX expression, 300  $\mu L$  of single cell suspension in staining buffer was permeabilised using BD permeablisation buffer (BD Biosciences UK). Permeabilised cells were re-suspended in 300  $\mu L$  of staining buffer

, the Pan Caspase NIR probe kit (Vergent ording to the manufacturer's instructions. The amily inhibitor VAD-FMK conjugated to a near as a marker that irreversibly binds to activated cells. Essentially, 300 µL of tumour single cell n staining buffer was centrifuged, the pellet re-L of 1XCAS-MAP NIR probe and incubated at room e dark for 1 h. Cells were washed three times by 400 RCF for 5 min in ice cold PBS and re-suspended in g buffer and analysed by flow cytometry. qRT-PCR was ate the expression of TMBIM1 in tumours as previously Briefly, RNA was extracted from microdissected slides ecoverAll Kit (Life Technologies, Paisley, UK). cDNA as carried out using the Superscript III First Strand cDNA it (Life Technologies, Paisley, UK) using the reverse primer f TMBIM1 (transmembrane BAX inhibitor motif containing 1) two housekeeping genes;18S rRNA and b-actin. qRT-PCR was out using the SYBR Green kit on the CFX96 instrument (BioRad, The qRT-PCR cycle was as follows: 95C for 3 min, 95C for 10 s, for 45 s for 40 cycles. For analysis, the geometric mean of 18S NA and b-actin was taken as the single housekeeping value. Statiscal comparison between the groups was carried out using two-way ANOVA with Bonferroni post-hoc analysis. The primers used to investigate the TMBIM1 expression are shown in the table below.

Sequence
CATCACTGCGGTGGTATCCA
GTATTGGAAGTAGAGCACAATGCTAGT
CGTGGGCCGCCCTAGGCACCA
TTGGCCTTAGGGTTCAGGGGGG
TGACTCAACACGGGAAACC
TCGCTCCACCAACTAAGAAC

# 2.8. Toxicity determination of MagO $_2$ MB-5FU and MagO $_2$ MB-RB conjugates

Healthy MF1 mice (8 weeks old) were randomly distributed into four groups (n = 10). Group 1 received no treatment; Groups 2 & 3 received a tail vein injection (100  $\mu$ L) of 5-FU (115 mM) or RB (1.03 mM) respectively and Group 4 received a tail vein injection (100 μL) containing a suspension of MagO<sub>2</sub>MB-RB/MagO<sub>2</sub>MB-5FU  $([MB] = 2.3 \times 10^8,$ [RB] = 570  $\pm$  15  $\mu$ M, = 503  $\pm$  7  $\mu$ M]) on Day 1 and Day 8. Pre-treatment tail vein bleeds (0.10 mL) were collected in lithium heparinised tubes on Day 0 with the post-treatment bleeds taken in a similar manner on Day 15. Blood samples were sent to CTDS Ltd. (Leeds, UK) for whole blood and plasma biochemical analysis. Urea, alanine aminotransferase (ALT), red blood cell (RBC), haemoglobin (Hb), haematocrit (HCT), mean corpuscular volume (MCV), mean corpuscular haemoglobin (MCH), mean corpuscular haemoglobin concentration (MCHC), platelet, white blood cell, neutrophil and lymphocyte levels were determined using accredited protocols. Following the Day 15 bleed, mice were then sacrificed and the liver and kidneys were surgically excised and placed in a formalin free tissue fixative solution (Sigma-Aldrich) for 24 h. It should be noted that the liver was chosen in these studies because it has been shown that MB are removed from circulation by that organ following intravenous administration. The tissue was then placed in an automated Leica

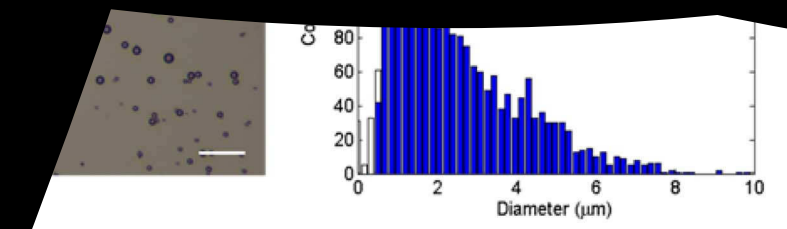
reticulin, Masson's trichrome, r required. The stained sections were reviewed historog ogists with expertise in liver and renal pathology. Liver architecture was initially assessed to establish if there was significant remodelling or fibrosis. The various liver compartments were subsequently examined for pathological changes. Portal tract and lobular inflammation grading was adapted from the Ishak (modified HAI) system [25]. Portal tract inflammation was graded numerically from 1 (none) to severe, affecting all portal tracts (5). Lobular inflammation was assessed at  $10 \times \text{mag}$ nification and graded as 1 (none) to 4 (severe, typically averaging > 10 foci per 10 × field). Fatty liver disease grading, referred to as steatosis/ steatohepatitis, was undertaken based on parameters assessed in the NAFLD activity score [26]. In short, steatosis was graded based on a visual estimate of the percentage of liver cells affected as 1 = noneor < 5%; 2 = mild, (5-33%); 3 = moderate (34-66%) and 4 = severe (> 67%). Kidney analysis was undertaken following a similar approach assessing the glomerular cellularity, glomerular basement membrane, tubular vacuolation, interstitial inflammation, interstitial fibrosis, vessel integrity and the collecting system. Statistical analysis was undertaken using a Student's t-test where the MagO<sub>2</sub>MB-RB/MagO<sub>2</sub>MB-5FU group was compared directly with the 5-FU, RB and untreated groups.

#### 3. Results and discussion

Magnetic microbubbles (MagMBs) were prepared by sonication of DBPC, DSPE-PEG(2000) and DSPE-PEG(2000)-biotin lipids in the presence of PFB gas and superparamagnetic iron oxide nanoparticles (NPs). The magnetic nanoparticle formulation comprised an iron oxide core with a lipid coating to facilitate incorporation of the magnetic nanoparticles into the MB shell. The PFB containing MagMBs (MagPFBMBs) produced had an average diameter of 1–2  $\mu$ m with a concentration of approximately 1  $\times$  10<sup>9</sup> MB/mL as determined by analysis of optical microscopy images (Fig. 1).

The iron content of the MagPFBMBs was also determined using atomic absorption spectroscopy and revealed the MBs contained 0.286 mg/10<sup>9</sup> MBs total iron content. Following isolation of the MagPFBMBs by centrifugation and surface coating with avidin, biotinylated Rose Bengal and biotinylated 5-FU were added to separate batches of the MagPFBMBs to generate Rose Bengal loaded MagPFBMBs (MagPFBMB-SFU) respectively. The PFB core gas was then exchanged with oxygen by sparging with pure oxygen gas for 2 min generating the MagO<sub>2</sub>MB-RB and MagO<sub>2</sub>MB-SFU conjugates (Scheme 1).

To determine the magnetic response of the MB platform, suspensions of MagMBs (1 mL) were placed in a syringe and pumped through a flow chamber (0.6 mL/min) with a fixed magnet (0.46 T) positioned on the underside of the flow chamber during the course of the experiment. A control study was also performed in the absence of a fixed magnet but under otherwise identical conditions. The number of MBs retained in the flow cell at the end of each experiment were counted and the results are shown in Fig. 2. A significant increase in the number of MBs (p < 0.01) was observed when the fixed magnet was present indicating the ability of the MagMBs to be retained against flow using an external magnetic field. Blood flow rates within the human body vary considerably depending on vessel type and size with blood leaving the aorta (2400 cm min 1) at a flow rate approximately 3 orders of magnitude greater than in capillaries  $(1.8 \text{ cm min}^{-1})$  [27]. In tumours, the increased viscous and geometrical resistance presented by the vasculature can compromise its blood flow, meaning the average velocity of



vessels can be an order of magnitude lower than in [28]. Therefore, the flow rate used in the current study ne upper limit of rates chosen to study tumour perfusing nich suggests that magnetic targeting may be effective in in the MBs in the tumour vasculature and allowing a greater to be destroyed in an applied acoustic field.

ler to retain a useful proportion (10%) of injected microat these blood flow rates, an estimated magnetic field gradient 5 T/m would provide sufficient force to capture superhagnetic particles flowing the capillary vessels [29]. When coning the possible translation of such technology to the clinic, both nsabdominal and endoscopic sources are viable methods for the elivery of magnetic fields to the pancreas. In the context of the above apillary flow rates, optimized permanent magnet designs with a volume of 1.02 cm3 [20] would be capable of targeting a tumour through the duodenal wall as part of an endoscopic probe, where the approximate distance to the head of the pancreas is in the region of 10 mm. In the case of transabdominal delivery, where the distances are more variable depending on the patient's body to mass index (BMI), the optimized permanent magnet volume would be in the region of 1.66 cm<sup>3</sup>, based on a distance of 50 mm from the outside of the abdomen to the pancreas. Even at flow rates 5 times higher than the capillary flow rate used above, the estimated field gradient to retain the same fraction of

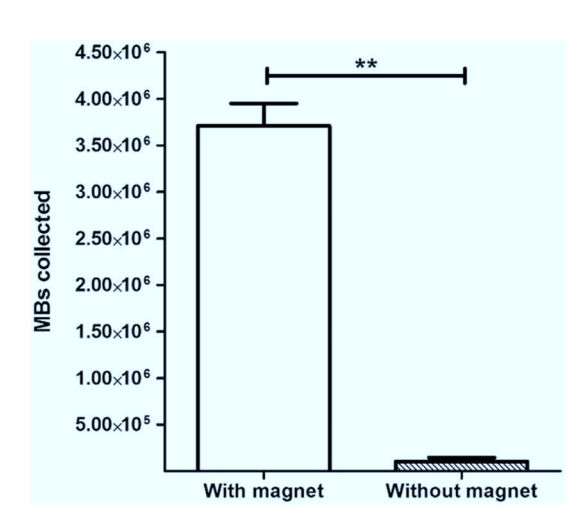
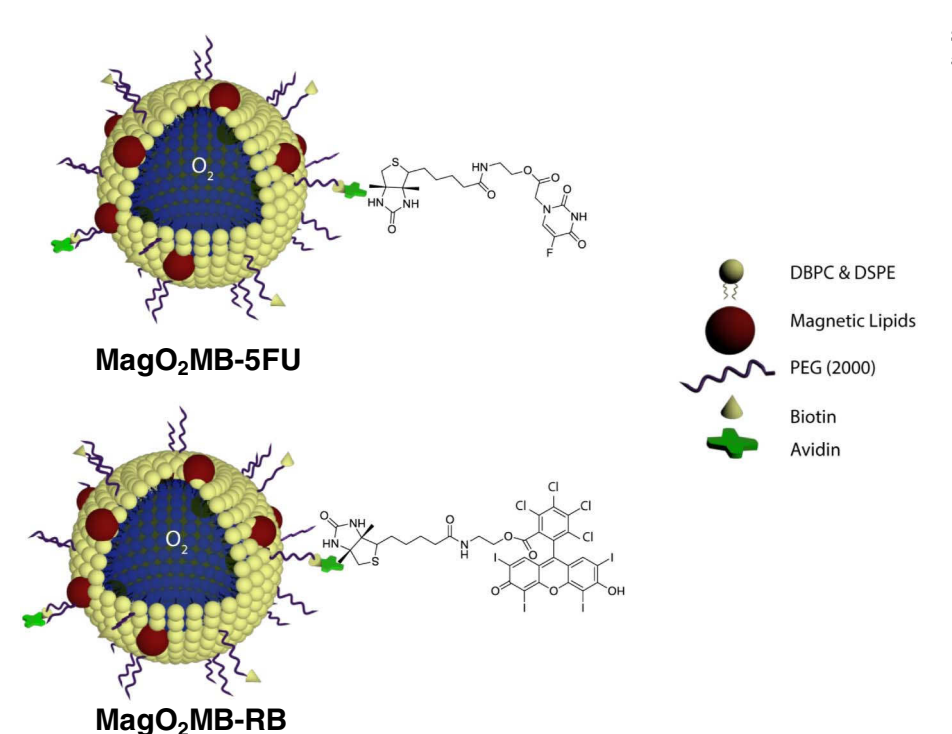
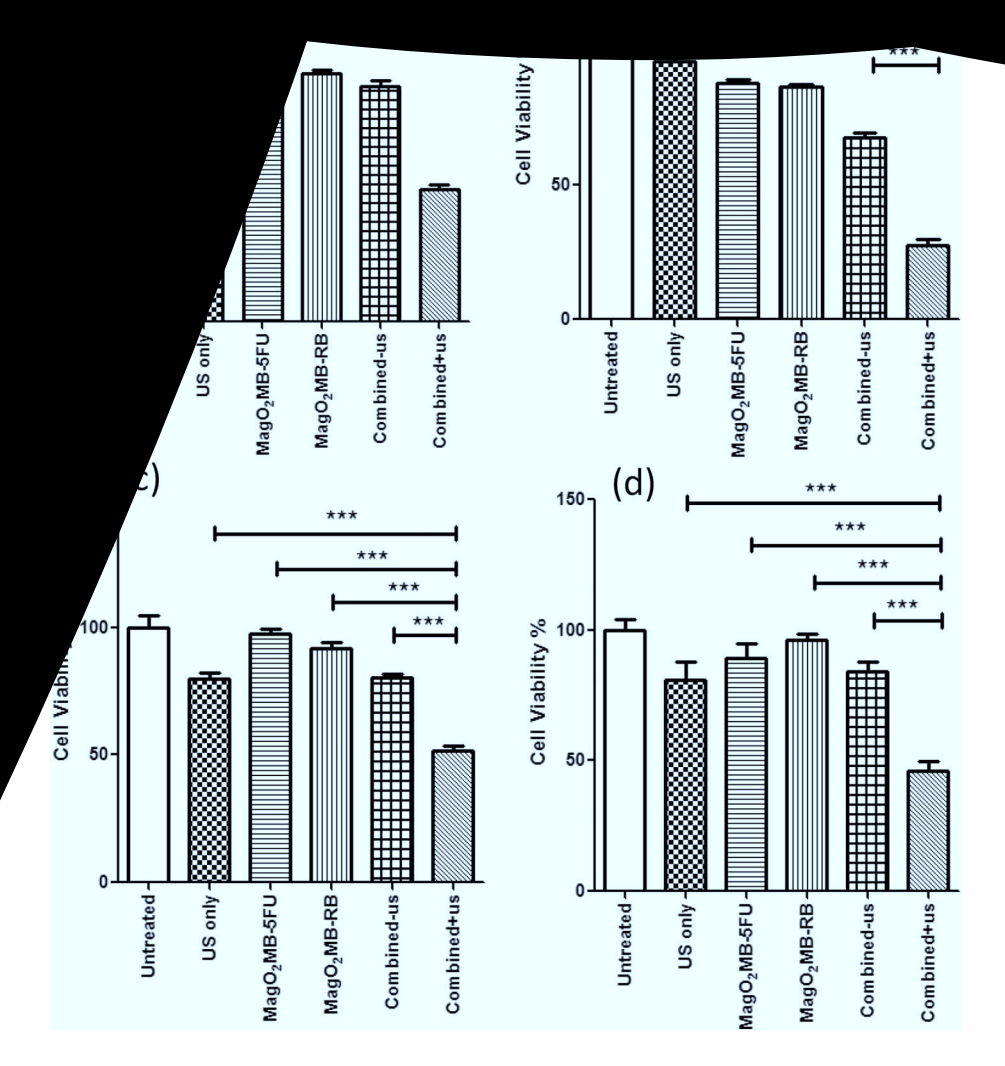


Fig. 2. Plot of MBs retained after injection through a flow-cell in the presence and absence of a fixed magnet.

MBs would be 2.48 T/m, requiring permanent magnet volumes in the region of  $1.5 \text{ cm}^3$  for an endoscopic device, which is readily achievable [30]. Given endoscopic ultrasound (EUS) analysis is a common

Scheme 1. Schematic representation of the  $MagO_2MB-5FU$  and  $MagO_2MB-RB$  conjugates.





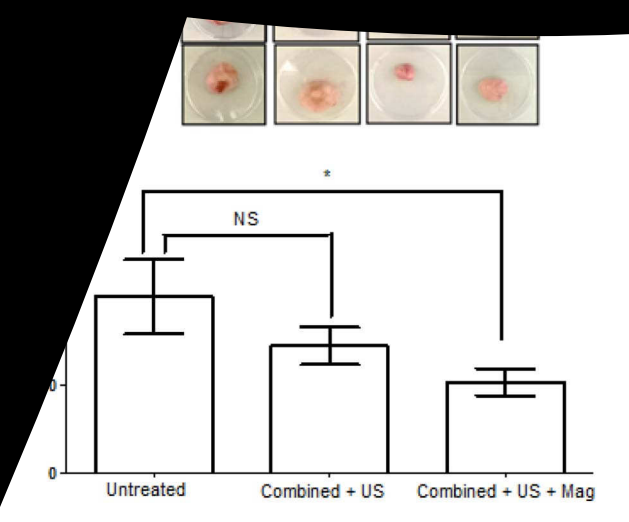
diagnostic tool used in staging pancreatic cancer, a EUS device configured to deliver both magnetic and ultrasonic fields is one possibility for the translation of this technology to clinic.

In a previous study, we demonstrated the benefit of combining Rose Bengal mediated SDT and 5-FU treatment, delivered using a non-magnetic O<sub>2</sub>MB platform, for the treatment of pancreatic cancer [6]. In the current study, we were keen to ensure that the presence of redox active Fe(II) and Fe(III) in the MB shell, would not hamper the effectiveness of SDT or 5-FU treatment. Therefore, the next step was to determine the toxicity of the combined treatment in a panel of pancreatic cancer cell lines. Human pancreatic BxPC-3, MiaPaCa-2 and Panc-01 cells were chosen as targets in addition to the T110299 cell line [31]. The latter was isolated from a primary pancreatic tumour in the KPC model (Ptf1a-Cre; LSL-Kras<sup>G12D</sup> and Ptf1aCre; LSL-Kras<sup>G12D</sup>; LSL-Trp<sup>53fl/R172H</sup> mice, respectively, that were back-crossed on a C57BL/6 background). The cells were seeded in 96 well plates and treated with a suspension of either MagO<sub>2</sub>MB-5FU, MagO<sub>2</sub>MB-RB or combined MagO<sub>2</sub>MB-5FU/MagO<sub>2</sub>MB-RB treatment in the presence of ultrasound. Untreated cells and cells treated with ultrasound only were used as controls.

The results are shown in Fig. 3 and reveal a significant reduction (p < 0.001) in cell viability for all cell lines that received combined SDT and 5-FU treatment with reductions > 50% relative to the untreated cells. In contrast, both the  $MagO_2MB$ -SFU and  $MagO_2MB$ -RB

formulations demonstrated only minor reductions (< 10%) in the absence of ultrasound treatment meaning it was possible to control the generation of cytotoxicity using the ultrasound stimulus. Therefore, these results suggest that application of ultrasound not only disrupts the MBs releasing the encapsulated  $O_2$  gas and the attached Rose Bengal/5-FU into the extracellular medium but also activates Rose Bengal leading to ROS generation and the observed cytotoxic effect [32]. It is also possible that application of the ultrasound could be enhancing the action of 5-FU by means of sonoporation. Indeed, it has been shown that this strategy can be employed to enhance the action of cancer chemotherapeutics by affording transient intracellular access of the drug via sonoporation [33].

While the in vitro cytotoxicity of the combined 5-FU/SDT treatment was encouraging, in vivo experiments are essential to identify the benefit of magnetic targeting. To this end, orthotopic human xenograft BxPC-3-Luc pancreatic tumours were established in SCID mice. Nineteen days following implantation the mice were randomly distributed into three groups (n = 4). Group 1 received no treatment; Group 2 received a MagO<sub>2</sub>MB-5FU/MagO<sub>2</sub>MB-RB suspension administered intravenously with the tumour region exposed to low-intensity ultrasound during and following injection for a total exposure of 3.5 min. Group 3 also received an IV injection of the MagO<sub>2</sub>MB-5FU/MagO<sub>2</sub>MB-RB suspension but in addition to ultrasound treatment, a



(a) Photographs of orthotopic BxPC-3 Luc tumours removed from SCID mice s following implantation after (i) no treatment (top), (ii) treatment with combined D<sub>2</sub>MB-RB and MagO<sub>2</sub>MB-FU plus ultrasound (middle) or (iii) treatment with gO<sub>2</sub>MB-RB and MagO<sub>2</sub>MB-FU plus ultrasound and magnet (bottom). Treatments were ministered on Day(s) 19, 20 and 21. (b) Plot of % change in tumour volume relative to intreated for mice treated with (ii) or (iii) above. \*p < 0.05 for (iii) compared to (i). A one-way ANOVA, post-Hoc test showed the same significance as above.

permanent magnet was also directed at the tumour during ultrasound treatment (3.5 min). Treatments were repeated on Days 20 and 21 with the mice sacrificed on Day 28 [34]. This treatment schedule was determined on the basis of a previous pilot study where multiple treatments in close succession were shown to be beneficial over a single treatment. In addition, as our primary goal is to use this technology as a neo-adjuvant treatment to downstage tumours in advance of surgery, aggressive treatment of the tumours with three successive administrations was the preferred choice and as the technology is targeted, significantly lower concentrations of RB and 5-FU are used compared to standard systemic administration. Once the mice were sacrificed, the tumours were surgically excised and volumes determined with the results for the three groups shown in Fig. 4.

A statistically significant reduction in tumour volume of 48.3% (p < 0.05) was observed for Group 3 relative to control Group 1, while for Group 2 an obvious downward trend in tumour volume (27.9%) was detected although this was not found to be statistically significant. This improvement in efficacy in the presence of a magnetic field could be due to more MBs being retained in the tumour microenvironment, so that ultrasound exposure can enable enhanced deposition of MB payloads and subsequent activation of the sensitiser. Although the latter would require verification by further experimentation, our suggestion is corroborated by the observation that, activated caspase and BAX protein levels were both significantly elevated in tumours harvested from Group 3, when compared to expression of those proteins in tumours from either of the other 2 groups (p < 0.05) (Fig. 5).

Increases in activated caspase and BAX protein levels are indicative of increased apoptosis and consistent with the increased treatment efficacy observed for Group 3. Although BAX and caspase were not significantly increased in Group 2, a trend in tumour size reduction was observed for this group (Fig. 4). In addition, previous studies have shown that ectopic BxPC-3 tumours receiving the combined treatment in the absence of a magnetic field resulted in decreased tumour size and expressed markers for increased apoptosis [6]. Although significant differences exist in the manner in which this and the previous study

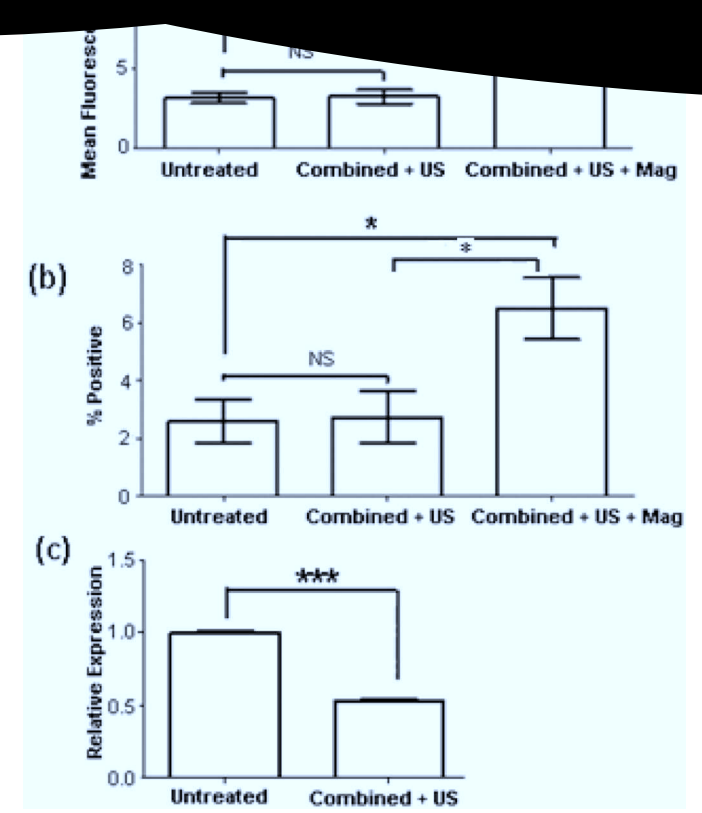


Fig. 5. (a) Plot showing presence of active caspase in single cell suspensions of tumours removed from SCID mice 38 days following implantation after treatment with (i) no treatment (left), (ii) treatment with combined MagO<sub>2</sub>MB-RB and MagO<sub>2</sub>MB-5FU plus ultrasound (middle) or (iii) treatment with MagO<sub>2</sub>MB-RB and MagO<sub>2</sub>MB-5FU plus ultrasound and magnet (right). Fluorescence indicates caspase activity which is reflective of apoptosis and was determined using the Pan Caspase probe (Pan Caspase NIR from Vergent Bioscience) via flow cytometry. Treatments were administered on Days 19, 20 and 21. (b) BAX protein expression of the same single cell suspensions via flow cytometry. \*p < 0.05 for (iii) compared to (i). (c) Relative expression of TMBIM1 in untreated control tumours and those receiving combined treatment. \*\*\*p < 0.001.

were performed both from the perspective of the model type (orthotopic vs. ectopic) and that of the dosing regimen (multiple vs. single), it was felt that the reduction 'trend' observed in Group 2 in the current study (Fig. 4) warranted further consideration. To this end, we have been able to use qRT-PCR analysis to demonstrate that TMBIM1 (encoding transmembrane BAX inhibitor motif containing 1) was significantly downregulated in tumours receiving the combined treatment in the absence of a magnetic field (Fig. 5). Since TMBIM1 is an inhibitor of BAX [35], its down regulation in these tumours could lead to enhanced BAX-mediated apoptosis without an observable change in BAX concentration. However, the authors do realise that the data presented in Figs. 4 and 5 were derived from tumours removed at a specific time point (9 days) following treatment and these data may differ if longer or shorter time-points were chosen. Continuing studies will include a more in-depth examination of gene expression at various time points in order to more clearly elucidate the interplay between both of these genes and their role in treatment-induced apoptosis.

It was also found during the above studies that animals receiving the magnetically-responsive platform did not suffer any overt adverse effects and no significant change in body weight was observed over the course of the experiment (Fig. 6a). To investigate the aspect of safety

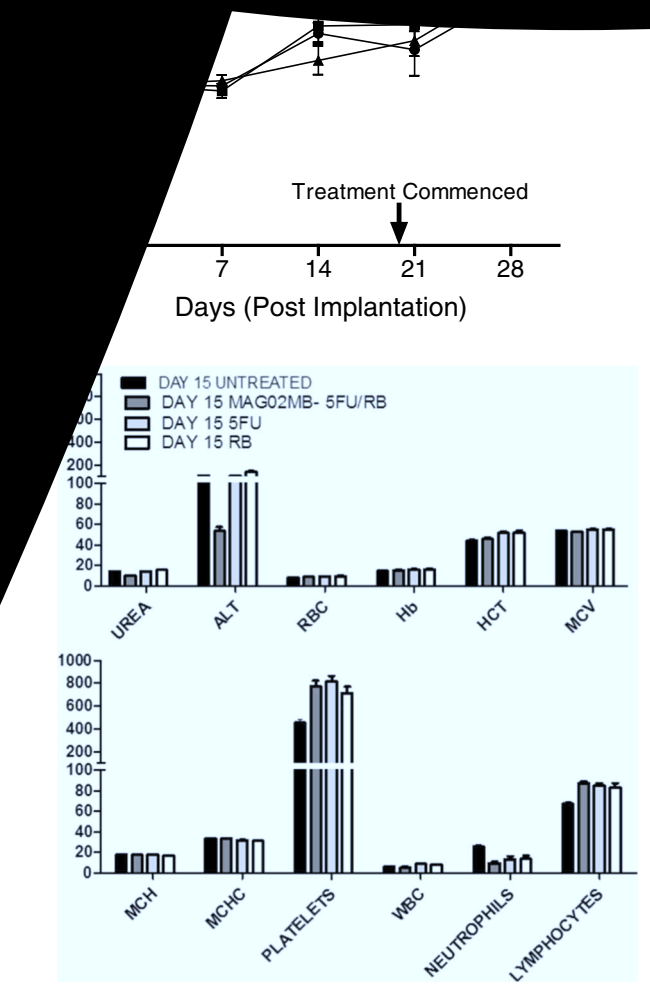


Fig. 6. (a) Average body weight of mice recorded following treatment with vehicle only (triangles), a suspension of MagO<sub>2</sub>MB-RB/MagO<sub>2</sub>MB-5FU + ultrasound (squares), or a suspension of MagO<sub>2</sub>MB-RB/MagO<sub>2</sub>MB-5FU + ultrasound + magnet (circles). (b) Whole blood and serum biochemistry analysis from healthy MF1 mice (i) untreated control, or treated with (ii) a suspension of MagO<sub>2</sub>MB-RB/MagO<sub>2</sub>MB-5FU, (iii) 5-FU alone, or (iv) RB alone.

further, a more detailed toxicology study was undertaken. This involved administering the MagO<sub>2</sub>MB-5FU/MagO<sub>2</sub>MB-RB suspension to 10 healthy non-tumour bearing MF1 mice by tail vein injection on Days 0 and 8. Similar experiments were undertaken involving MF1 mice treated with 5-FU or Rose Bengal alone at concentrations higher than those present on the MagMBs to reflect clinical doses, while untreated animals served as a control group. Blood samples were harvested from each group of animals on Day 15 and analysed for a range of key biochemical markers (Fig. 6b). No major differences in profile were observed between the MagO2MB-5FU/MagO2MB-RB group and the other groups that would raise any concern regarding toxicity of the combined MB-based treatment. Indeed ALT activity, which is a measure of liver function, was lower in the MagO2MB-5FU/MagO2MB-RB group compared to the other groups. While there was an increase in platelet and lymphocyte levels for the MagO<sub>2</sub>MB-5FU/MagO<sub>2</sub>MB-RB group relative to the untreated group, levels were also raised in 5-FU and Rose Bengal treated animals and the differences between these groups were not significant.

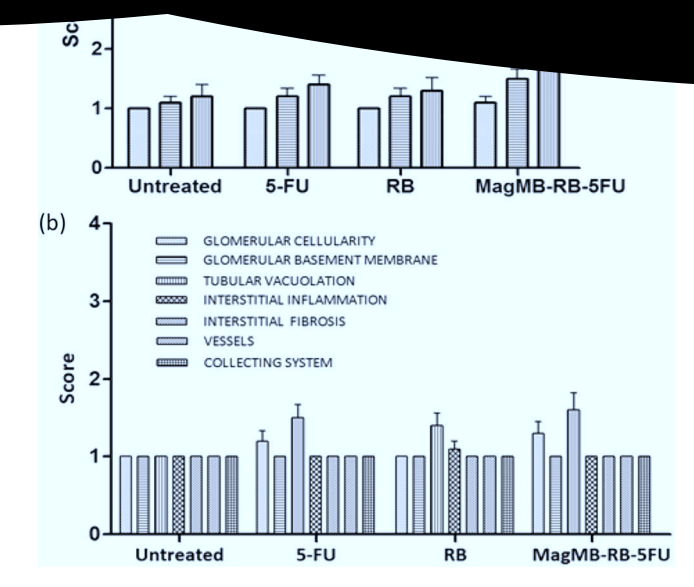


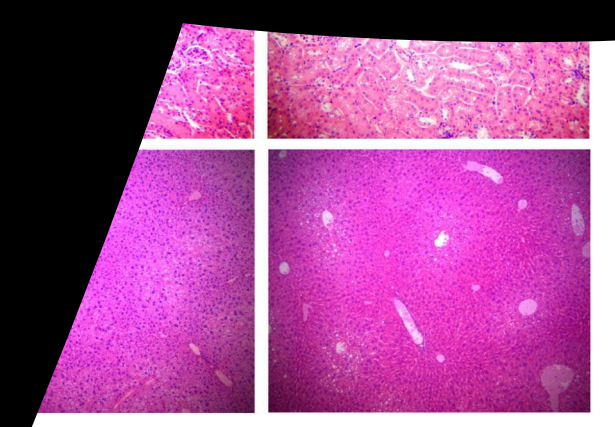
Fig. 7. Scoring for sections of (a) liver and (b) kidney following (i) no treatment, or treatment with (ii) 5-FU alone, (iii) RB alone, or (iv) a suspension of  $MagO_2MB-RB/MagO_2MB-5FU$  conjugates. Portal inflammation scored 1–5 while all other parameters were scored from 1 to 4. In each case a score of 1 = normal.

Similarly, there was evidence of mild neutropenia in the three treatment groups relative to the untreated group, but again the difference between the  $MagO_2MB$ -SFU/MagO\_2MB-RB group and the 5-FU and RB groups was not significant. Furthermore, histological analysis of liver and kidney sections removed post-mortem on Day 16 also revealed no significant changes between the  $MagO_2MB$ -SFU/MagO\_2MB-RB group and the 5-FU or RB treated groups (Fig. 7).

There was evidence of a slight increase in liver steatosis score for the MagO<sub>2</sub>MB-5FU/MagO<sub>2</sub>MB-RB group but this was not significant when compared to the 5-FU or RB groups. Liver steatosis, also known as fatty liver disease, is normally a consequence of dietary or lifestyle habits but can also be influenced by certain chemotherapeutic drugs including antimetabolites [36]. The slight increase in score for the MagO<sub>2</sub>MB-5FU/MagO<sub>2</sub>MB-RB group relative to 5-FU or RB may be due to the uptake and metabolism of the lipid component of the MBs and on that basis is likely a transient change of limited clinical significance. Analysis of kidney sections showed slightly raised levels of glomerular cellularity and tubular vacuolation for the MagO2MB-5FU/MagO2MB-RB group, but again these levels were also raised in the 5-FU and RB groups and the differences were non-significant. Some of the tubular vacuolation may have been artefactual, possibly fixation related, as it was observed in both treated and untreated groups. It must be stressed, however, that any effect observed in the liver or kidney histology analysis was deemed to be mild and in no case did the mean score exceed 2. Collectively, these results indicate the potential of O<sub>2</sub>MagMBs as a safe and effective platform for the delivery of combined antimetabolite and SDT treatment of pancreatic cancer (Fig. 8).

### 4. Conclusions

Magnetically responsive MBs were successfully prepared and shown to be retained at a target site in the presence of an externally applied magnetic field. When decorated with the sensitiser Rose Bengal and the antimetabolite 5-FU, the MagO<sub>2</sub>MB conjugates produced reductions of > 50% in the viability of four pancreatic cancer cell lines upon



esentative H & E stained microscope images of liver (top) and kidney ctions taken from animals sacrificed on Day 15 following treatment with a of MagO<sub>2</sub>MB-RB/MagO<sub>2</sub>MB-5FU (right) or untreated (left).

ure to relatively low intensity ultrasound. The combined applian of external magnetic and ultrasound fields during IV delivery of MagO<sub>2</sub>MB conjugates resulted in a 48.3% reduction in orthotopic ancreatic tumour volumes 9 days after treatment relative to the control group, while the application of ultrasound alone resulted in a reduction of only 27.9%. In addition, a significant increase in apoptosis was observed in tumours that were treated with the MagMB conjugates and exposed to both magnetic and ultrasonic fields when compared to the ultrasound alone or untreated groups. These results highlight the potential of using a combination of magnetic and ultrasonic fields to retain and disrupt MBs in the tumour vasculature. The results also confirm the effectiveness of combined sonodynamic/antimetabolite therapy delivered using the MagO<sub>2</sub>MB platform as a safe, highly targeted and efficacious treatment for pancreatic cancer.

### Acknowledgements

JFC thanks Norbrook Laboratories Ltd. for an endowed chair. ES and JO thank the Engineering and Physical Sciences Research Council for support through grant EP/I021795/1. EB thanks the Research Councils UK Digital Economy Programme for support through grant EP/G036861/1 (Oxford Centre for Doctoral Training in Healthcare Innovation). We also thank Prof. Jens Siveke at Medizinische Klinik; Klinikum rechts der Isar; Technische Universität München; Munich, Germany for the KPC cell line. We acknowledge Dangoor Education for their supporting RH in this work.

### References

- S. Badger, J. Brant, C. Jones, J. McClements, M. Loughrey, M. Taylor, T. Diamond, L. McKie, The role of surgery for pancreatic cancer: a 12-year review of patient outcome, Ulster Med. J. 79 (2010) 70–75.
- [2] J. Li, M.G. Wientjes, J.L. Au, Pancreatic cancer: pathobiology, treatment options, and drug delivery, AAPS J. 12 (2010) 223–232.
- [3] M.H. Katz, P.W. Pisters, D.B. Evans, C.C. Sun, J.E. Lee, J.B. Fleming, J.N. Vauthey, E.K. Abdalla, C.H. Crane, R.A. Wolff, Borderline resectable pancreatic cancer: the importance of this emerging stage of disease, J. Am. Coll. Surg. 206 (2008) 833–846.
- [4] M. Tachezy, F. Gebauer, C. Petersen, D. Arnold, M. Trepel, K. Wegscheider, P. Schafhausen, M. Bockhorn, J.R. Izbicki, E. Yekebas, Sequential neoadjuvant chemoradiotherapy (CRT) followed by curative surgery vs. primary surgery alone for resectable, non-metastasized pancreatic adenocarcinoma: NEOPA-a randomized multicenter phase III study (NCT01900327, DRKS00003893, ISRCTN82191749), BMC Cancer 14 (2014) 1.
- [5] C. Hamill, SBRT pre-operatively for borderline resectable pancreatic cancer, UK Clinical Trials Gateway website, 2014 (Study ID Numbers:OCTO\_054).

- [9] G. Dimcevski, S. Kotopouns, A. Molven, H. Sorbye, E. McCormack, A Itums. crobubbles to enhance gemcitabine treatment of inoperable pancrease. Release 243 (2016) 172–181.
- [10] S. Kotopoulis, G. Dimcevski, O. Helge Gilja, D. Hoem, M. Postema, Treatment of human pancreatic cancer using combined ultrasound, microbubbles, and gemcitabine: a clinical case study. Med. Phys. 40 (2013).
- [11] S. Umemura, N. Yumita, R. Nishigaki, K. Umemura, Mechanism of cell damage by ultrasound in combination with hematoporphyrin, Jap. J. Cancer Res. 81 (1990) 962–966.
- [12] H. Chen, J.H. Hwang, Ultrasound-targeted microbubble destruction for chemotherapeutic drug delivery to solid tumors. J. Therapeutic Ultrasound 1 (2013) 1.
- [13] S. Hernot, A.L. Klibanov, Microbubbles in ultrasound-triggered drug and gene delivery, Adv. Drug Deliv. Rev. 60 (2008) 1153–1166.
- [14] M.M.A. Valenzuela, J.W. Neidigh, N.R. Wall, Antimetabolite treatment for pancreatic cancer, Chemotherapy 3 (2014).
- [15] D. Costley, C. Mc Ewan, C. Fowley, A.P. McHale, J. Atchison, N. Nomikou, J.F. Callan, Treating cancer with sonodynamic therapy: a review, Int. J. Hyperth. 31 (2015) 107–117.
- [16] N. Nomikou, C. Fowley, N.M. Byrne, B. McCaughan, A.P. McHale, J.F. Callan, Microbubble–sonosensitiser conjugates as therapeutics in sonodynamic therapy, Chem. Commun. 48 (2012) 8332–8334.
- [17] C. McEwan, J. Owen, E. Stride, C. Fowley, H. Nesbitt, D. Cochrane, C.C. Coussios, M. Borden, N. Nomikou, A.P. McHale, Oxygen carrying microbubbles for enhanced sonodynamic therapy of hypoxic tumours, J. Control. Release 203 (2015) 51–56.
- [18] Y. Gao, C.U. Chan, Q. Gu, X. Lin, W. Zhang, D.C.L. Yeo, A.M. Alsema, M. Arora, M.S.K. Chong, P. Shi, Controlled nanoparticle release from stable magnetic microbubble oscillations, NPG Asia Mater. 8 (2016) e260.
- [19] J. Owen, P. Rademeyer, D. Chung, Q. Cheng, D. Holroyd, C. Coussios, P. Friend, Q.A. Pankhurst, E. Stride, Magnetic targeting of microbubbles against physiologically relevant flow conditions, Interface Focus 5 (2015) 20150001.
- [20] C. Crake, J. Owen, S. Smart, C. Coviello, C. Coussios, R. Carlisle, E. Stride, Enhancement and passive acoustic mapping of cavitation from fluorescently tagged magnetic resonance-visible magnetic microbubbles in vivo, Ultrasound Med. Biol. 42 (2016) 3022–3036.
- [21] J. Ciccolini, C. Mercier, M. Blachon, R. Favre, A. Durand, B. Lacarelle, A simple and rapid high-performance liquid chromatographic (HPLC) method for 5-fluorouracil (5-FU) assay in plasma and possible detection of patients with impaired dihydropyrimidine dehydrogenase (DPD) activity, J. Clin. Pharm. Ther. 29 (2004) 307–315.
- [22] L.C. Barnsley, D. Carugo, J. Owen, E. Stride, Halbach arrays consisting of cubic elements optimised for high field gradients in magnetic drug targeting applications, Phys. Med. Biol. 60 (2015) 8303.
- [23] A. McHale, L. McHale, Use of a tetrazolium based colorimetric assay in assessing photoradiation therapy in vitro, Cancer Lett. 41 (1988) 315–321.
- [24] L.C. Barnsley, D. Carugo, E. Stride, Optimized shapes of magnetic arrays for drug targeting applications, J. Phys. D 49 (2016) 225501.
- [25] K. Ishak, A. Baptista, L. Bianchi, F. Callea, J. De Groote, F. Gudat, H. Denk, V. Desmet, G. Korb, R.N. MacSween, Histological grading and staging of chronic hepatitis, J. Hepatol. 22 (1995) 696–699.
- [26] D.E. Kleiner, E.M. Brunt, M. Van Natta, C. Behling, M.J. Contos, O.W. Cummings, L.D. Ferrell, Y. Liu, M.S. Torbenson, A. Unalp-Arida, Design and validation of a histological scoring system for nonalcoholic fatty liver disease, Hepatology 41 (2005) 1313–1321.
- [27] E.N. Marieb, K. Hoehn, The cardiovascular system: blood vessels, human anatomy, Physiology (2013) 703–720.
- [28] R.K. Jain, T. Stylianopoulos, Delivering nanomedicine to solid tumors, Nat. Rev. Clin. Oncol. 7 (2010) 653–664.
- [29] L.C. Barnsley, D. Carugo, M. Aron, E. Stride, Understanding the dynamics of superparamagnetic particles under the influence of high field gradient arrays, Phys. Med. Biol. 62 (2017) 2333.
- [30] T. Krings, J. Finney, P. Niggemann, P. Reinacher, N. Lück, A. Drexler, J. Lovell, A. Meyer, R. Sehra, P. Schauerte, Magnetic versus manual guidewire manipulation in neuroradiology: in vitro results, Neuroradiology 48 (2006) 394–401.
- [31] P. Duewell, E. Beller, S.V. Kirchleitner, T. Adunka, H. Bourhis, J. Siveke, D. Mayr, S. Kobold, S. Endres, M. Schnurr, Targeted activation of melanoma differentiation-associated protein 5 (MDA5) for immunotherapy of pancreatic carcinoma, Oncoimmunology 4 (2015) e1029698.
- [32] We have previously demonstrated in Ref 6 the effects of combined RB and 5-FU treatment (5 μM and 100 μM respectively) as free agents (i.e. not as MB conjugates) to cause between 20–30% reduction in viability in BxPC-3, MiaPaCa-2 and Panc-01 cell lines.
- [33] N. Nomikou, A.P. McHale, Exploiting ultrasound-mediated effects in delivering targeted, site-specific cancer therapy, Cancer Lett. 296 (2010) 133–143.
  [34] The treatment schedule and termination date was informed by an earlier pilot study and
- [34] The treatment schedule and termination date was informed by an earlier pilot study and supported by bioluminescent imaging.
- [35] D.A. Lisak, T. Schacht, V. Enders, J. Habicht, S. Kiviluoto, J. Schneider, N. Henke, G. Bultynck, A. Methner, The transmembrane Bax inhibitor motif (TMBIM) containing protein family: tissue expression, intracellular localization and effects on the ER CA 2 filling state, Biochim. Biophys. Acta (BBA)-Mol. Cell Res. 1853 (2015) 2104–2114.
- [36] K. Miyake, K. Hayakawa, M. Nishino, T. Morimoto, S. Mukaihara, Effects of oral 5-fluorouracil drugs on hepatic fat content in patients with colon cancer 1, Acad. Radiol. 12 (2005) 722–727.